Comparative study of the properties of the Cu-M-O thin films (M=In and Sb)

Nadia Chaglabou
Photovoltaic and Semiconductor Materials, Laboratory, ENIT, Tunisia

Mounir Kanzari
Photovoltaic and Semiconductor Materials Laboratory, ENIT, Tunisia

Abstract

The purpose of this work is to investigate and compare structural and optical properties of the Cu-M-O thin films (M=In and Sb). Samples were prepared via sequential thermal vacuum deposition of Cu and M on glass substrates after what they were heated in vacuum at 200°C for 1 hour followed by an annealing at 400 °C in air atmosphere. XRD of Cu/In system show the presence of Cu_9In_{11} phase after annealing in vacuum and In_2O_3, CuO and Cu phases after annealing in air atmosphere. For Cu/Sb system, we note the formation of Cu_2Sb and Sb after annealing in vacuum, and the presence of α-Sb_2O_4 ,Sb_2O_3 and CuO phases after annealing in air atmosphere. The optical study indicated that the absorption coefficient of Cu-M-O thin films in all cases is in the range 10^4-10^5 cm^{-1}. The electrical measurements show a conversion from a metallic phase to the semiconductor phase after annealing.

1. Introduction

Recently, a great deal of interest has been focused on transparent conducting oxides (TCOs) due to their wide application in transparent electronic devices such as transparent electrodes for liquid crystal displays (LCDs), organic light emitting diodes (OLEDs) and solar cells [1,2]. Among binary compounds that have attracted much attention as new materials for TCO films we cite ZnO, MgO, In_2O_3, Ga_2O_3, and SnO_2 [3–5]. ZnO, In_2O_3, and SnO_2 TCO films all have n-type conductivity in nature [6–10]. Oxides of copper are also attracting renewed interest as promising TCO. Two common forms of copper oxide are Cu_2O and CuO. Both the CuO and Cu_2O are p-type semiconductors [11]. TCOs based on a Cu+ based system were also examined as $CuMO_2$ (M=Al,Ga,In) [12],[13] and [14], $SrCu_2O_2$[15], LnCuOS (Ln=lanthanide) [16,17] and systems Ag-Cu-O [18], Cu-In-O [19] and Cu-Sb-O [20] .

In this paper, we report the preparation and characterization of Cu-M-O system (M=Sb or In). The effect of the annealing in air atmosphere of the sample, the order of deposition of materials (Cu and M or M and Cu)) and the number of couples (Cu/M/Cu/M…) on structural, optical and electrical properties was studied.

2. Experimental procedures

The starting intermetallic multilayer systems used in this study, were prepared according the previous paper [20] by vacuum thermal evaporation in a sequential mode of pure (99.999%) Cu and M (M=Sb or In) and a thermal annealing. Thermal evaporation sources were used which can be controlled either by the crucible temperature or by the source power. The distance from crucible to sample holder was 12 cm. The pressure during evaporation was maintained between 10^{-5} and 10^{-6} Torr. The glass substrates were previously cleaned with washing agents commercial (detergent, acetone, ethanol and de-ionized water) before being introduced into the vacuum system. The substrate temperature was measured using a chromel-alumel thermocouple during the evaporation process. All obtained samples were prepared by two processes: an annealing at 200 °C for 1h in vacuum (10^{-6} Torr) followed by an annealing at 400 °C in air atmosphere at different times. The crystalline structure of the synthesized films was investigated by using X-ray diffraction (XRD) with a Philips D8 equipment using a monochromator CuKα radiation (λ=1.54056Å) at room temperature.

Optical transmission and reflection for the samples were measured at normal incidence with an UV–visible-NIR Shimadzu spectrophotometer equipped with an integrated sphere in the wavelength range 300-1800 nm. Conductivity types of the samples were measured with the hot probe method.

3. Results and discussion

3.1. Structural properties

The structural properties of the intermetallic multilayer systems $(Cu/M)^{j=1,2,3}$ and $(M/Cu)^{j=1,2,3}$

(M=Sb or In) for both films after annealing in vacuum at 200°C for 1 hour and films after annealing in air atmosphere at 400°C for different times were analyzed by XRD. The XRD spectra of the intermetallic multilayer systems $(Cu/M)^{j=1,2,3}$ and $(M/Cu)^{j=1,2,3}$ (M=Sb or In) annealed in vacuum at 200°C for 1 hour are presented in Figure 1 and Figure 2 .

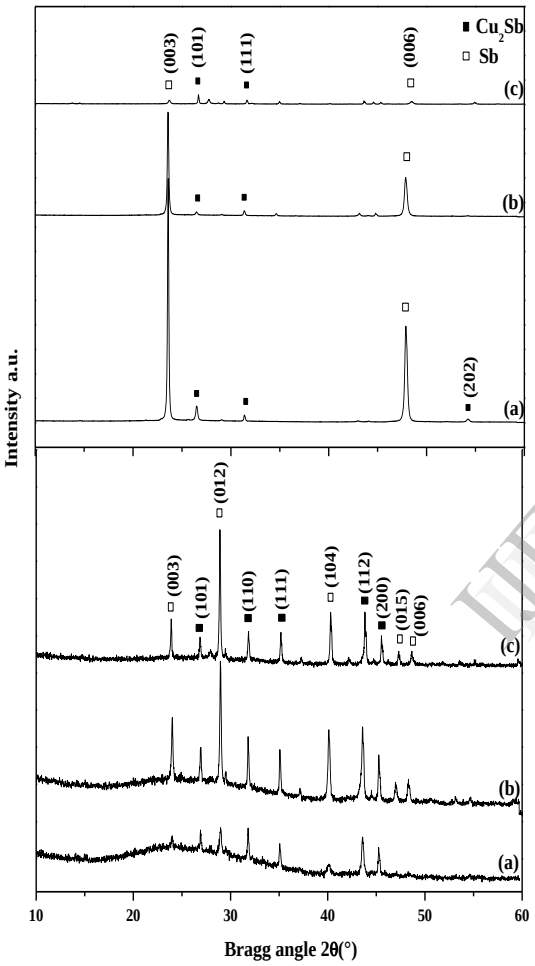

Figure 1. XRD patterns of $(Cu/Sb)^{j=1}$ (a), $(Cu/Sb)^{j=2}$ (b), $(Cu/Sb)j^{=3}$ (c), $(Sb/Cu)^{j=1}$ (d), $(Sb/Cu)^{j=2}$ (e) and $(Sb/Cu)^{j=3}$ (f) annealed in vacuum at 200°C for 1 hour

It is clear from Figure 1 that the patterns of $(Cu/Sb)^{j=1,2,3}$ and $(Sb/Cu)^{j=1,2,3}$ showed a mixture of Cu_2Sb and antimony phases, and the sequences starting with antimony, i.e. $(Sb/Cu)^{j=1}$ (d), $(Sb/Cu)^{j=2}$ (e) and $(Sb/Cu)^{j=3}$ (f) appear most crystallized that the sequences starting with copper i.e. $(Cu/Sb)^{j=1}$ (a), $(Cu/Sb)^{j=2}$ (b) and $(Cu/Sb)^{j=3}$ (c).

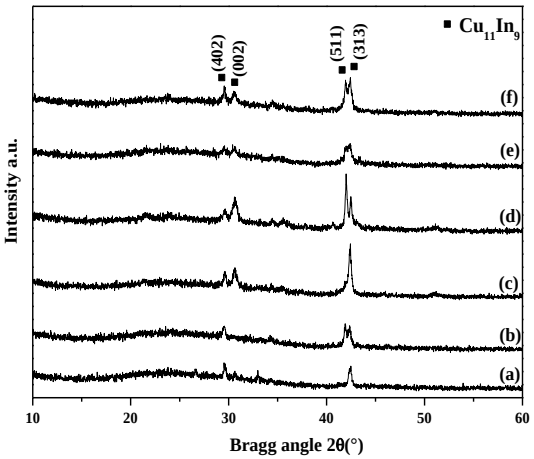

Figure 2. XRD patterns of $(Cu/In)^{j=1}$(a), $(In /Cu)^{j=1}$ (b), $(Cu/ In)^{j=2}$(c), $(In /Cu)^{j=2}$ (d), $(Cu/ In)^{j=3}$(e) and $(In /Cu)^{j=3}$ (f) annealed in vacuum at 200°C for 1 hour

The patterns of $(Cu/In)^{j=1,2,3}$ and $(In/Cu)^{j=1,2,3}$ show that all peaks were identified at monoclinic $Cu_{11}In_9$ phase (Figure 2), and the order of deposition of materials (Cu and In or In and Cu) has no effect on the crystallinity of the samples.

Figure 3 and Figure 4 show the results of our XRD measurements after annealing in air atmosphere at 400°C for different times of the intermetallic multilayer systems $(Cu/M)^{j=1,2,3}$ and $(M/Cu)^{j=1,2,3}$ (M=Sb or In). It can be seen that the structural properties of the (Cu/In) annealed system are very similar for all the sequences (Figure 3), whereas the structural properties of annealed intermetallic multilayer system Cu/Sb strongly depend on the sequence (Figure 4). For the (Cu/In) system, the patterns of $(Cu/In)^{j=1,2,3}$ and $(In/Cu)^{j=1,2,3}$ show In_2O_3 as main crystalline phase with a preferential orientation (222) in addition to CuO and a small amount of metallic copper for all annealed multilayer systems excepted $(Cu/In)^{j=1}$ (a) and $(Cu/In)^{j=2}$ (b) we note non existence of metallic copper. For the (Cu/Sb) system (Figure 4), the patterns of $(Cu/Sb)^{j=1}$ (a), $(Cu/Sb)^{j=2}$ (b), $(Cu/Sb)^{j=3}$ (c) and $(Sb/Cu)^{j=3}$ (f) annealed in air atmosphere, show two phases, α-Sb_2O_4 and CuO, and it is clear that no crystalline phases of copper or antimony metal were detected by X-ray diffraction, indicating a total oxidation of the intermetallic multilayer systems. For the rest of the sequences i.e. $(Sb/Cu)^{j=1}$ (d) and $(Sb/Cu)^{j=2}$ (e) annealed in air atmosphere, two phases Sb_2O_3 and CuO were detected with a dominant peak corresponding to the Sb_2O_3 phase with a preferential orientation (222). We can note also the presence of antimony phase

only for $(Sb/Cu)^{j=1}$ (d) after annealing in air atmosphere at 400°C for 3h.

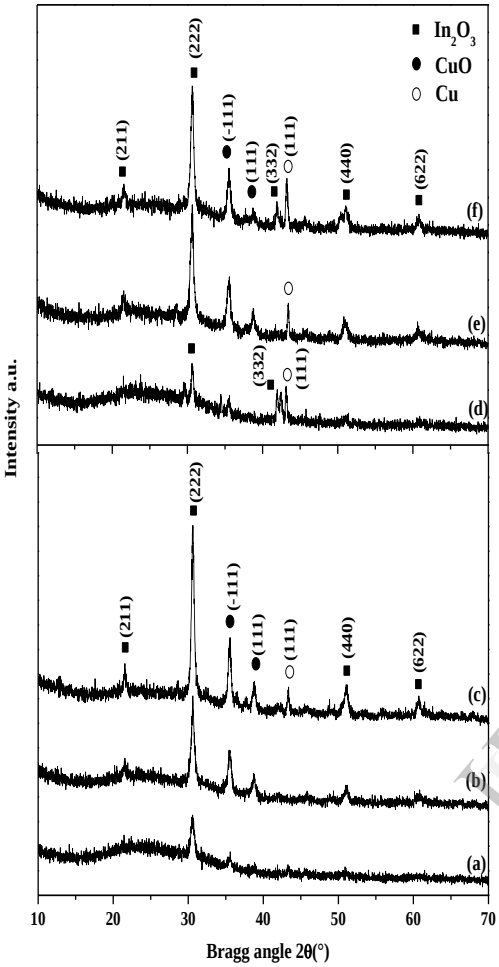

Figure 3. XRD patterns of $(Cu/In)^{j=1}$ (a), $(Cu/ In)^{j=2}$ (b), $(Cu/ In)^{j=3}$ (c), $(In /Cu)^{j=1}$ (d), $(In /Cu)^{j=2}$ (e) and $(In /Cu)^{j=3}$ (f) annealed in air atmosphere at 400°C

3.2. Optical properties

Figure 5-8 show the spectral distribution both of the transmission T and the reflection R at normal incidence for the annealed intermetallic multilayer systems $(Cu/M)^{j=1,2,3}$ and $(M/Cu)^{j=1,2,3}$ (M=Sb or In) in air atmosphere at 400°C.

Optical transmission of Cu/Sb system was about 60% except the samples $(Sb/Cu)^{j=1}$ (b) and $(Sb/Cu)^{j=2}$ (d) annealed in air atmosphere, when antimony films are deposited firstly (Figure 5). It is clear from Figure 7, that after annealing in air atmosphere at 400°C the optical transmission of the sequences starting with copper, i.e. $(Cu/In)^{j=1}$ (a), $(Cu/In)^{j=2}$ (c) and $(Cu/In)^{j=3}$ (e) is most important that optical transmission of the sequences starting with indium, i.e. $(In/Cu)^{j=1}$ (b), $(In/Cu)^{j=2}$ and $(In/Cu)^{j=3}$ (f) in particular the sequence$(Cu/In)^{j=2}$ (c) when the optical transmission reaches 60% .

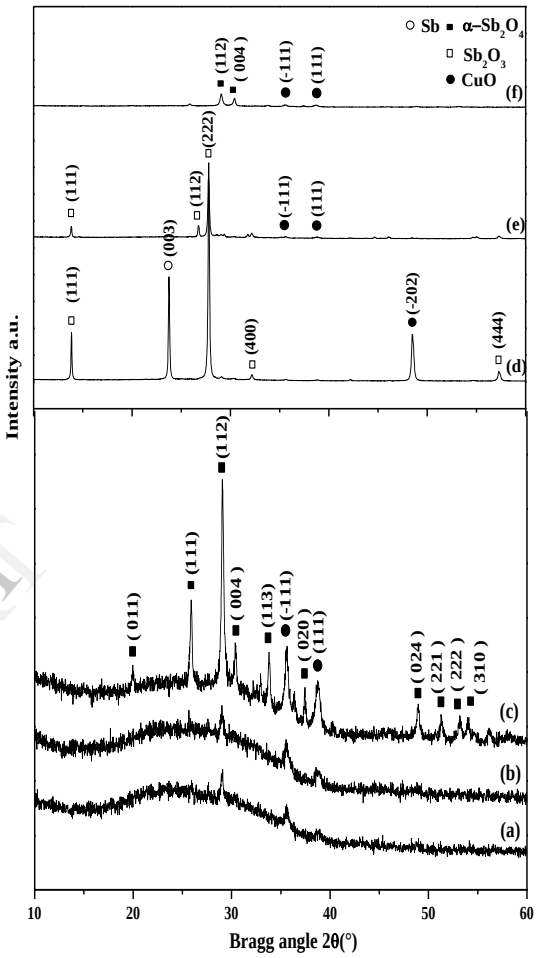

Figure 4. XRD patterns of $(Cu/Sb)^{j=1}$ (a), $(Cu/ Sb)^{j=2}$ (b), $(Cu/ Sb)^{j=3}$ (c), $(Sb /Cu)^{j=1}$ (d), $(Sb /Cu)^{j=2}$ (e) and $(Sb /Cu)^{j=3}$ (f) annealed in air atmosphere at 400°C

The optical absorption coefficients were evaluated from the transmission and reflection data taken at 300K using the formula [21];

$$\alpha = \frac{1}{d}\ln\left[\frac{(1-R)^2}{T}\right]$$

Where α is the absorption coefficient in cm^{-1}, d is the thickness of the film, T and R are the transmission and reflectance, respectively. Fig 9 and Fig 10 show the absorption coefficients as a function of the photon energy. It can be seen that all the films have relatively high absorption

coefficient (10^4-10^5 cm^{-1}) in the visible range and near-IR spectral range.

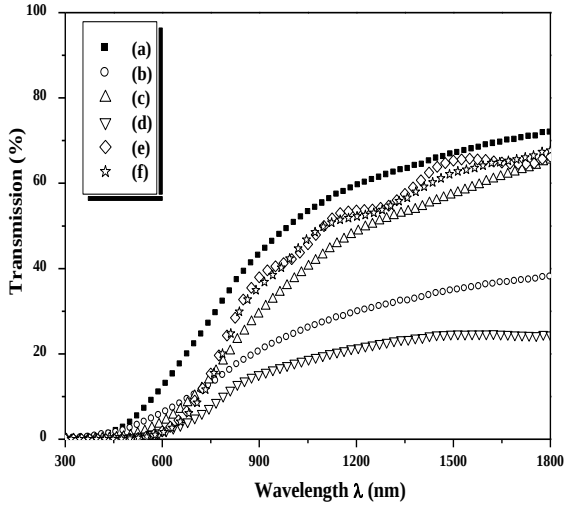

Figure 5. Optical transmission of $(Cu/Sb)^{j=1}$ (a), $(Sb/Cu)^{j=1}$ (b), $(Cu/Sb)^{j=2}$ (c), $(Sb/Cu)^{j=2}$ (d), $(Cu/Sb)^{j=3}$ (e), and $(Sb/Cu)^{j=3}$ (f) annealed in air atmosphere at 400°C

On other hand, it is clear that the absorption coefficient, α, decreases as the number of couples Cu/Sb (or Sb/Cu) increases for Cu/Sb system. The absorption coefficient α is related to the energy gap Eg according to the equation [22]:

$$\alpha h\nu = A(h\nu - Eg)^n$$

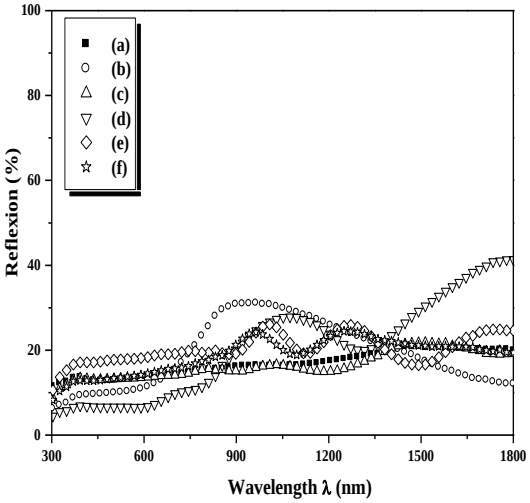

Figure 6. Optical reflection of $(Cu/Sb)^{j=1}$ (a), $(Sb/Cu)^{j=1}$ (b), $(Cu/Sb)^{j=2}$ (c), $(Sb/Cu)^{j=2}$ (d),$(Cu/Sb)^{j=3}$ (e), and $(Sb/Cu)^{j=3}$ (f) annealedin air atmosphere at 400°C

Where A is a constant, h is the Plank constant and n is an exponent that depends on the type of transition. For direct allowed transition n=1/2 and for indirect allowed transition n=2.

The value of the direct and indirect energy gap for films are obtained by extrapolating the linear regions of the $(\alpha h\nu)^2$ and $(\alpha h\nu)^{1/2}$ versus hν curve to the horizontal photon energy axis.

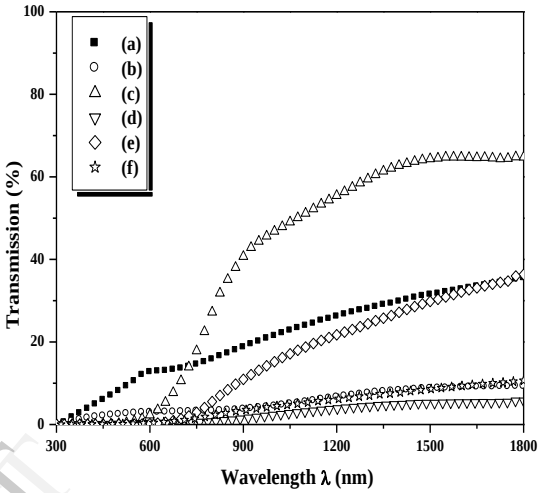

Figure 7. Optical transmission of $(Cu/In)^{j=1}$ (a), $(In/Cu)j^{=1}$ (b), $(Cu/In)^{j=2}$ (c), $(In/Cu)^{j=2}$ (d),$(Cu/In)^{j=3}$ (e), and $(In/Cu)^{j=3}$ (f) annealed in air atmosphere at 400°C

For the (Cu/Sb) system annealed in air atmosphere, two direct allowed transitions, Eg_1 and Eg_2, were founded for each sample which corresponds, respectively, to the band gap of copper oxide and antimony oxide phases. Indeed it has been shown [23-26] that CuO present a band gap of 1.3-2.1eV and the band gap of α-Sb2O4 is in general higher than the band gap of Sb_2O_3 [27]. We note also, for the (Cu/In) system annealed in air atmosphere , the presence of two direct band gaps, Eg_1 and Eg_2, for each sample, associated respectively, to the band gap of CuO [23-26] and In_2O_3 [28] phases.

Optical parameters determined for Cu–Sb–O and Cu–In–O systems were summarized in the table 1 and table 2.

For the (Cu/Sb) system annealed in air atmosphere, table 1 show a decrease of the values of the direct energy with the increase of the number of couples. It's similar for (Cu/In) system annealed in air atmosphere (table 2) ; the increase of the number of couples has contributed in the decrease of the values of the direct energy.

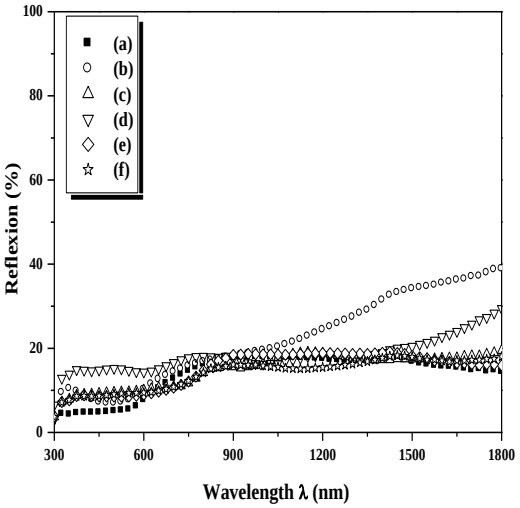

Figure 8. Optical reflection of $(Cu/In)^{j=1}$ (a),$(In/Cu)^{j=1}$ (b), $(Cu/In)^{j=2}$ (c), $(In/Cu)^{j=2}$ (d), $(Cu/In)^{j=3}$ (e), and $(In/Cu)^{j=3}$ (f) annealed in air atmosphere at 400°C

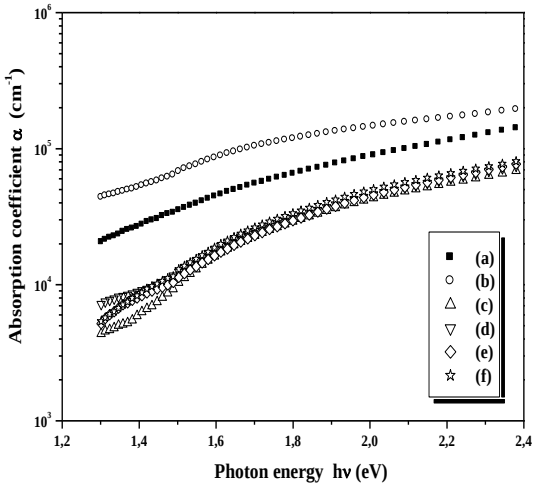

Figure 9. Absorption coefficient spectra of $(Cu/Sb)^{j=1}$ (a), $(Sb/Cu)^{j=1}$ (b), $(Cu/Sb)^{j=2}$ (c), $(Sb/Cu)^{j=2}$ (d), $(Cu/Sb)^{j=3}$ (e), and $(Sb/Cu)^{j=3}$ (f) annealed in air atmosphere at 400°C

Table 1. Optical parameters of $(Cu/Sb)^{j=1}$(a), $(Sb/Cu)^{j=1}$ (b), $(Cu/Sb)^{j=2}$(c), $(Sb/Cu)^{j=2}$ (d), $(Cu/Sb)^{j=3}$ (e), and $(Sb/Cu)^{j=3}$ (f) annealed in air atmosphere at 400°C.

Samples	Thickness (nm)	n_c	Eg (eV)	
			Eg_1	Eg_2
(a)	192	1.94	1.49	2.95
(b)	170	2.12	1.48	2.75
(c)	571	1.96	1.50	2.80
(d)	550	2.41	1.50	2.60
(e)	717	2.14	1.50	2.20
(f)	701	2.11	1.49	2.20

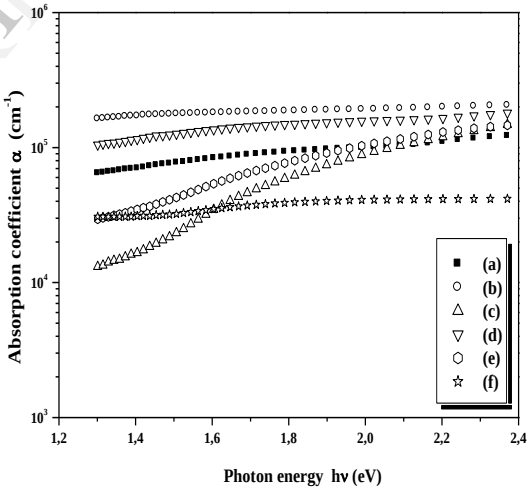

Figure 10. Absorption coefficient spectra $(Cu/In)^{j=1}$ (a), $(In/Cu)^{j=1}$ (b), $(Cu/In)^{j=2}$ (c), $(In/Cu)^{j=2}$ (d), $(Cu/In)^{j=3}$ (e), and $(In/Cu)^{j=3}$ (f) annealed in air atmosphere at 400°

Table 2. Optical parameters of $(Cu/In)^{j=1}$ (a), $(In/Cu)^{j=1}$ (b), $(Cu/In)^{j=2}$ (c), $(In/Cu)^{j=2}$ (d), $(Cu/In)^{j=3}$ (e), and $(In/Cu)^{j=3}$ (f) annealed in air atmosphere at 400°C.

Samples	Thickness (nm)	n_c	Eg (eV)	
			Eg_1	Eg_2
(a)	188	1.91	1.50	3.72
(b)	162	2.13	1.50	3.71
(c)	550	1.92	1.51	2.37
(d)	535	1.94	1.48	2.21
(e)	675	1.95	1.51	1.87
(f)	670	1.90	1.50	2.30

3.3 Electrical properties

For the configuration of the electrical measurements, two gold electrodes were subsequently deposited as shown in figure 11.The (Cu/Sb) system annealed in air atmosphere at 400 °C are highly compensated except the samples $(Cu/Sb)^{j=3}$ and $(Sb/Cu)^{j=3}$ which exhibit p-type conductivity. For The (Cu/In) system annealed in air atmosphere at 400 °C, all the sequences starting

with indium, i.e. $(In/Cu)^{j=1}$, $(In /Cu)^{j=2}$ and $(In/Cu)^{j=3}$ show p-type conductivity, and the sequences starting with copper show n-type conductivity with the exception of $(Cu/In)^{j=3}$ which confirmed also a p-type conductivity. So, it is clear that only the films deprived of copper phase after annealing in air atmosphere (figure 3) show n-type conductivity.

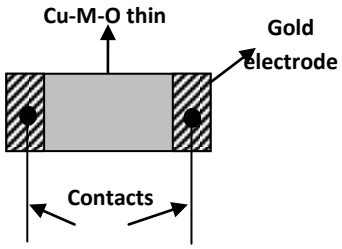

Figure 11. Layer configuration for the electrical measurements

4. Conclusion

Cu–Sb–O and Cu–In–O systems have been obtained in two stages: sequential evaporation of metal precursors (Cu and Sb or In), and annealing in a vacuum (10^{-6} Torr) followed by an annealing in air atmosphere. The most important conclusion pointed out after this study is that the nature of the metal M (antimony or indium), the order of deposition of materials and the number of couples affect structural, optical and electrical properties.

X-ray diffraction analysis confirmed that antimony improve the crystallinity of thin films compared in indium, and for Cu-Sb-O system, the best crystallinity is obtained in the case when copper films are deposited onto antimony films. For Cu-In-O system, the order of deposition of materials (Cu and In or In and Cu) has no effect on the crystallinity of the samples. The optical parameters (refractive index, n, absorption coefficient and optical band gap, Eg) of the films were determined by simple calculations using the transmission and reflection spectra. The Cu-M-O thin films have two direct band gap energies: between 1.48–1.50 eV and 2.20-2.95 eV for Cu-Sb-O system and in the ranges of 1.48–1.51 eV and 1.87-3.72 eV for Cu-In-O system. After annealing in air atmosphere, Cu-Sb-O system is highly compensated except the samples $(Cu/Sb)^{j=3}$ and $(Sb/Cu)^{j=3}$ which exhibit p-type conductivity and for Cu-In-O system some sample are p-type and some are n-type. The origin of the p-type conductivity is probably due to the role of the state of Cu oxidation or/and the state of Sb (or In) oxidation which affect the conductivity of the films. So the Cu-M-O thin films (M=In or Sb) are interest candidates for technological applications such photovoltaic since antimony, indium and copper are more abundant in nature and their prices are lower than other metallic materials.

5. References

[1] E. Fortunato, D. Ginley, H. Hosono, D. C. Paine, *MRS Bulletin*, 32 (2007) 242.
[2] E. Fortunato, L. Raniero, L. Silva, A. Goncalves, A. Pimen tel, P. Barquinha, H. Aguas, L. Pereira, G. Goncalves, I.Ferreira, E. Elangovan, R. Martins, *Solar Energy Materials and Solar Cells*, 92 (2008) 1605.
[3] N. Ueda, T. Omada, N. Hikuma, K. Ueda, H. Kawazoe, *Appl. Phys. Lett*. 61 (1992) 1954.
[4] T. Omata, U. Ueda, N. Hikuma, K. Ueda, H. Kawazoe, *Appl. Phys. Lett*. 62 (1993) 499.
[5] T. Ninami, H. Sonohara, T. Kakumu, S. Takada, Jpn. *J. Appl. Phys*. 34 (1995) L971.
[6] K.L. Chopra, S. Major, D.K. Pandya, *Thin Solid Film* 102 (1983) 1.
[7] I. Hamberg, C.G. Granqvist, *J. Appl. Phys*. 60 (1986) R123.
[8] C.G. Granqvist, *Appl. Phys*. A53 (1991) 83.
[9] H. Sato, T. Minami, S. Takata, T. Miyata, M. Ishii, *Thin Solid Film* 236 (1993) 14.
[10] F. Zhu, P. Jennings, J. Cornish, G. Hefter, K. Luczak, *Solar Energy Mater. Solar Cells* 49 (1997) 163.
[11] S.C. Ray, *Sol. Energy Mater. Sol. Cells* 68 (2001) 307.
[12] H. Kawazoe, M. Yasukawa, H. Hyodo, M. Kurita, H. Yana gi and H. Hosono. *Nature* 389 (1997) 939–940.
[13] K. Ueda, T. Hase, H. Yanagi, H. Kawazoe, H. Hosono, H. Ohta, M. Orita and M. Hirano. *J. Appl. Phys*. 893 (2001)1790.
[14] H. Yanagi, T. Hase, S. Ibuki, K. Ueda and H. Hosono, *Appl. Phys. Lett*. 78 (2001) 1583.
[15] A. Kudo, H. Yanagi, H. Hosono and H. Kawazoe, *Appl. Phys. Lett*. 73 (1998), p. 220.
[16] H. Hiramatsu, K. Ueda, H. Ohta, M. Orita, M. Hirano and H. Hosono, *Appl. Phys. Lett*. 81 (2002), p. 598.
[17] H. Hiramatsu, H. Ohta, T. Suzuki, C. Honjo, Y. Ikuhara, K. Ueda, T. Kamiya, M. Hirano and H. Hosono, *Cryst. Growth Des*. 4 (2004), p. 301.
[18] J.F. Pierson , E. Rolin, C. Clement-Gendarme, C. Petit Jean, D. Horwat, *Applied Surface Science* 254 (2008) 6590– 6594.
[19] N. Khemiri, F. Chaffar Akkari, M. Kanzari, and B. Rezig. *Phys. Stat. Sol*. (a) 205, No. 8, 1952–1956 (2008).
[20] N.Chaglabou, F.Chaffar Akkari, and M.Kanzari *Phys.Stat.Sol* (c) 7, No. 9, 2321–2325 (2010).
[21] D. E. Milovzorov, A. M. Ali, T. Inokuma, Y. Kurata, T. Suzuki, and S. Hasegawa, *Thin Solid Films* 382, 47 (2001).
[22] E. A. Davis and N. F. Mott, *Philos*. Mag. 22, 903 (1970).
[23] S.C. Ray, *Sol Energy Mater Sol Cells* 68 (2001) 307.
[24] A.A. Ogwu, E. Bouquerel, O. Ademosu, S. Moh, E. Crossan and F. Placido, *J Phys D Appl Phys* 38(2005)266.

[25] J.F. Pierson, A. Thobor-Keck and A. Billard, *Appl Surf Sci* 210 (2003), p. 359.
[26] F. Marabelli, G.B. Parravicini and F. Salghetti-Drioli, *Phys Rev* B 52 (1995) 1433
[27] P. Charton, P. Thomas, P. Armand. *Journal of Non-Crystalline Solids* 321 (2003) 81–88.
[28] L. Gupta, A. Mansingh and P. K. Srivastava, *Thin Solid Films*, 176 (1989) 33.